RESEARCH MEMORANDUM

TWO-DIMENSIONAL WIND-TUNNEL INVESTIGATION AT HIGH REYNOLDS NUMBERS OF TWO SYMMETRICAL CIRCULAR-ARC AIRFOIL SECTIONS WITH HIGH-LIFT DEVICES

By

William J. Underwood and Robert J. Nuber

Langley Memorial Aeronautical Laboratory
Langley Field, Va.

NATIONAL ADVISORY COMMITTEE FOR AERONAUTICS

WASHINGTON

March 12, 1947

NATIONAL ADVISORY COMMITTEE FOR AERONAUTICS

RESEARCH MEMORANDUM

TWO-DIMENSIONAL WIND-TUNNEL INVESTIGATION AT HIGH REYNOLDS NUMBERS OF TWO SYMMETRICAL CIRCULAR-ARC AIRFOIL SECTIONS WITH HIGH-LIFT DEVICES

By William J. Underwood and Robert J. Nuber

SUMMARY

An investigation was made of two symmetrical circular-arc airfoils of 6 and 10 percent thickness and equipped with leading-edge and trailing-edge high-lift devices. The high-lift devices consisted of a 0.20-chord plain trailing-edge flap, a 0.15-chord drooped-nose flap and a 0.10-chord leading-edge extensible flap. The section lift, pitching-moment, and some drag characteristics of the two supersonic airfoils tested at high Reynolds numbers and low Mach numbers ($M \leq 0.14$) with the various high-lift devices are presented.

Maximum section lift coefficients of 1.95 and 2.03 were obtained at a Reynolds number of 6×10^6 for the optimum combination of drooped-nose and plain flaps for the 6- and 10-percent-thick airfoils, respectively. The optimum combinations of flap deflections for the 6- and 10-percent-thick airfoils were found to be $\delta_n = 30^\circ$, $\delta_f = 60^\circ$, and $\delta_n = 36^\circ$, $\delta_f = 60^\circ$, respectively, where δ_n represents the drooped nose and δ_f the plain trailing-edge flap deflections. The results for the 10-percent-thick airfoil with the plain trailing-edge flap deflected 60° indicate no important changes in the maximum section lift coefficient with small departures from the optimum drooped-nose flap deflection. With the flaps neutral the maximum section lift coefficients for the 6- and 10-percent-thick airfoils were 0.73 and 0.67, respectively. The results also indicated that the scale effects on the maximum section lift coefficient were, in general, negligible over the range of Reynolds number from 3×10^6 to 18×10^6.

The section pitching-moment characteristics indicated that the aerodynamic center was ahead of the quarter-chord point and moved

toward the leading edge when any of the high-lift devices was deflected or extended.

Deflecting the drooped-nose flap was more effective in extending the low-drag range to higher section lift coefficients than deflecting the plain flap.

INTRODUCTION

The present rapid rate of development of airplanes that are expected to fly successfully in the transonic and supersonic speed ranges has focused great attention on the characteristics of airfoils having sharp leading edges. The principal requirement of these airfoils is a low drag in the appropriate speed range. If the airplane is also expected to land safely or to fly satisfactorily in the low-speed range, however, it is also necessary that means be provided for increasing the naturally low maximum lift of the sharp-edged airfoils. An investigation has been made accordingly in the Langley two-dimensional low-turbulence pressure tunnel of the improvements in maximum section lift coefficient that can be obtained by the use of simple high-lift devices. This wind tunnel enables both the Reynolds number and the Mach number appropriate to the landing condition for a typical airplane to be approximated simultaneously. The airfoils used were of symmetrical circular-arc shapes and were 6 and 10 percent thick. Each airfoil was equipped with a 20-percent-chord plain trailing-edge flap, a 15-percent-chord drooped-nose flap, and alternately a 10-percent-chord leading-edge extensible flap.

The section lift and pitching-moment characteristics were determined for both airfoils with the high-lift devices deflected individually and in combination with one another. The section drag characteristics were obtained for the 6-percent-thick airfoil with the flaps partly deflected as low-drag-control flaps and for both airfoils with the flaps neutral.

COEFFICIENTS AND SYMBOLS

c_l section lift coefficient $\left(\frac{l}{q_o c}\right)$

c_d section drag coefficient $\left(\frac{d}{q_o c}\right)$

$c_{m_{c/4}}$ section pitching-moment coefficient about the quarter chord $\left(\frac{m_{c/4}}{q_o c^2}\right)$

$c_{m_{a.c.}}$ section pitching-moment coefficient about the aerodynamic center $\left(\frac{m_{a.c.}}{q_o c^2}\right)$

where

l lift per unit span

d drag per unit span

m pitching moment per unit span

c chord of airfoil with all flaps neutral

q_o free-stream dynamic pressure $\left(\frac{\rho_o V_o^2}{2}\right)$

ρ_o free-stream density

V_o free-stream velocity

and

α_o section angle of attack, degrees

δ_n drooped-nose flap deflection, degrees, positive downward

δ_f plain flap deflection, degrees, positive downward

R Reynolds number

$\Delta\alpha_{c_{l_{max}}}$ increment of section angle of attack at maximum lift due to flap deflection

$\Delta c_{l_{max}}$ increment of maximum section lift coefficient due to flap deflection

DESIGNATION OF SUPERSONIC AIRFOILS

With the advent of supersonic airplanes, airfoils with sharp leading edges and varying shapes have been designed. Two supersonic airfoils of circular-arc shape with thicknesses

of 6 and 10 percent are discussed herein and are designated NACA 2S-(50)(03)-(50)(03) and NACA 2S-(50)(05)-(50)(05), respectively. The significance of these designations is indicated in the following example:

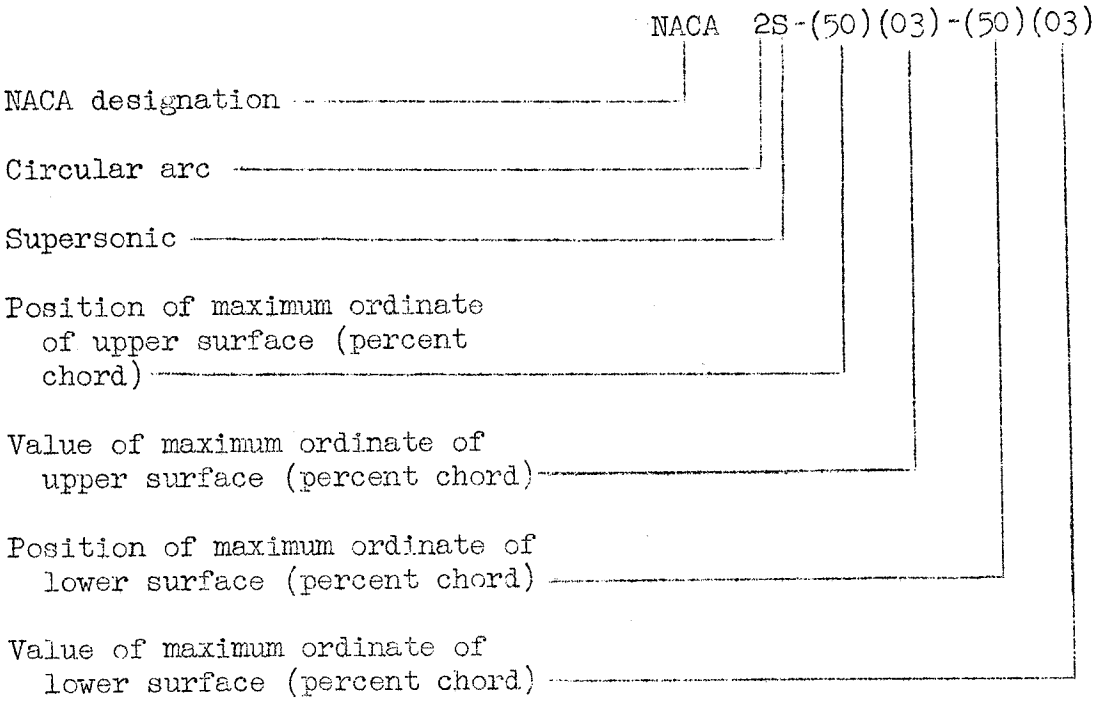

The designation 2S-(50)(03)-(50)(03), therefore, denotes a symmetrical circular-arc airfoil with a maximum thickness of 6 percent at midchord. Ordinates of the 6- and 10-percent-thick circular-arc airfoils are given in tables I and II, respectively.

MODELS

Both of the circular-arc-airfoil models had a 24-inch chord and a 35.5-inch span and were made of steel. The flaps of the 6-percent-thick airfoil were made of brass and those of the 10-percent-thick airfoil were made of duralumin. Sketches of the models are presented as figure 1. The 0.20-chord plain flap and the 0.15-chord drooped-nose flap were pivoted on leaf hinges mounted flush with the lower surface. The leading-edge flap was a 0.10-chord extension of the upper surface arc ahead of the normal leading edge of the plain airfoil. Model end plates as shown in figure 2 were used to facilitate setting the deflection of the drooped-nose and plain flaps. The models were designed so that plain flap deflections δ_f up to 60° and drooped-nose flap deflections δ_n

up to 50° could be obtained. The flaps were sealed at the hinge line by having the flap skirt in rubbing contact with the flap. When the plain flap of the 6-percent-thick airfoil was deflected beyond 50°, the gap between the flap and skirt was sealed with modeling clay to prevent leakage.

For all tests, the surfaces of the models were finished with No. 400 carborundum paper to produce smooth surfaces; slight discontinuities, however, still existed at the leaf hinges on the lower surfaces and at the line of contact between the flaps and flap skirts.

TESTS

Tests of the two models were made in the Langley two-dimensional low-turbulence pressure tunnel. The tests included measurements at a Reynolds number of 6×10^6 of airfoil lift and pitching moment for each model with the high-lift devices deflected either individually or in conjunction with one another.

At Reynolds numbers of 3×10^6 and 9×10^6 the lift characteristics of both models were obtained with the flaps neutral and with the drooped-nose and plain flaps deflected simultaneously to 30° and 60°, respectively. At these Reynolds numbers the lift characteristics of the NACA 2S-(50)(05)-(50)(05) airfoil were also determined with the drooped-nose and plain flaps deflected simultaneously to 36° and 60°, respectively. A further investigation of the lift characteristics at 14×10^6 and 18×10^6 was made for the NACA 2S-(50)(05)-(50)(05) airfoil with the flaps neutral and with the drooped-nose and the plain flaps deflected to 36° and 60°, respectively. Drag measurements of each model for the flaps-neutral condition were obtained by wake surveys at Reynolds numbers of 3×10^6, 6×10^6, and 9×10^6.

At Reynolds numbers of 3×10^6, 6×10^6, and 9×10^6 the Mach number was substantially constant at 0.10. At Reynolds numbers of 14×10^6 and 18×10^6 the Mach numbers were 0.12 and 0.14, respectively.

The lift and drag characteristics of the NACA 2S-(50)(03)-(50)(03) airfoil with the drooped-nose and plain flaps deflected as low-drag-control flaps were obtained at a Reynolds number of 2.1×10^6 in the Langley two-dimensional low-turbulence tunnel.

For these tests, the high-lift devices, both individually or in combination with one another, were deflected through a range of flap deflections from 0° to 10°. Evaluation of the section drag characteristics of the NACA 2S(50)(03)-(50)(03) airfoil with the high-lift devices deflected more than 10° by the wake-survey method (the only method available) proved impractical because of large spanwise variations in drag that occurred when the flow was partly separated.

The airfoil lift, drag, and pitching moment were measured and corrected to free-air conditions by the methods described in reference 1.

Lift measurements of the models with the flaps neutral, with and without model end plates, (figs. 2 and 3) indicated that the model end plates had no significant effect on the measured characteristics.

RESULTS AND DISCUSSION

Plain airfoils.-The aerodynamic section characteristics of the 6- and 10-percent-thick symmetrical circular-arc airfoils with the flaps neutral are presented in figure 4.

The maximum section lift coefficients are 0.73 and 0.67 for the 6- and 10-percent-thick airfoils, respectively. This decrease in maximum section lift coefficient with increasing airfoil thickness is opposite to the trends that may be shown from the data of NACA 6-series airfoils (reference 1) through the same thickness range and may be explained as follows: As the thickness of the NACA 6-series airfoils is increased from 6 to 10 percent, the corresponding increase in the airfoil leading-edge radius results in improved air-flow conditions around the leading edge at the high angles of attack. The increase in trailing-edge angle that results with increasing thickness tends to decrease the maximum section lift coefficient due to an increase in boundary-layer thickness on the upper surface. The favorable effect of a large leading-edge radius appears to predominate in this thickness range for the NACA 6-series airfoils and higher values of maximum lift are produced. For the circular-arc airfoils, however, the leading edges of both the 6- and 10-percent thick airfoils are sharp and the air-flow conditions around the leading edges at high angles of attack are about the same. The effect of an increase in trailing-edge angle with increasing thickness results in a decrease of maximum lift.

The lift-curve slopes are 0.097 and 0.090 for the 6- and 10-percent-thick airfoils, respectively. Because the air-flow conditions around the leading edge of both circular-arc airfoils are probably very nearly alike through the complete range of angles of attack, the thicker boundary layer of the 10-percent-thick airfoil caused the decrease in the lift-curve slope.

The slope of the lift curve for the 10-percent-thick airfoil was measured at small positive or negative values of the lift coefficient to avoid including the slight jog in the lift curve that occurs near zero lift. This discontinuity is probably due to an extensive thickening of the boundary layer on the low pressure surface resulting from an increase in the trailing-edge angle. A similar phenomenon may have existed on the 6-percent thick airfoil but was not of sufficient magnitude to cause a significant jog in the lift curve. The data (fig. 4) show no appreciable scale effect on the lift characteristics of either circular-arc airfoil with the flaps neutral through the range of Reynolds numbers investigated.

The variation of the quarter-chord pitching-moment coefficient of both the 6- and 10-percent-thick circular-arc airfoils indicates a forward position of the aerodynamic center with respect to the quarter-chord point of the airfoil. This variation of the pitching moment probably results from the relative thickening of the boundary layer near the trailing edge on the upper surface with increasing angle of attack. The aerodynamic center of the 10-percent-thick airfoil is more forward than that of the 6-percent-thick airfoil. This shift in aerodynamic-center position is attributed to the increase in trailing-edge angle or thickening of 0.90c. (See reference 2.) As is usually true when an airfoil stalls, the center of pressure of the circular-arc airfoils moves toward the rear and the quarter-chord moment coefficient increases negatively in the normal manner. The small negative pitching moment of both models at zero lift is attributed to asymmetrical loading resulting from very small model irregularities.

With airfoils having sharp leading edges, the drag coefficient increases fairly rapidly as the angle of attack departs from zero. In general, the drag coefficients decrease with increasing Reynolds number in approximately the manner expected for fully developed turbulent flow on both surfaces. In the case of the 6-percent-thick airfoil, however, laminar flow apparently was obtained over a fairly extensive portion of the upper surface at zero and negative angles of attack at Reynolds numbers of 3×10^6 and 6×10^6, as indicated by the lower drag for these conditions as compared with the drag obtained at a Reynolds number of 9×10^6.

Airfoils with high-lift devices.- The lift and pitching-moment characteristics of the two symmetrical circular-arc airfoils for various deflections of the leading-edge and trailing-edge high-lift devices deflected individually are presented in figures 5 to 7.

The maximum section lift coefficients of the 6- and 10-percent-thick airfoils increased as the 0.20-chord plain flap was deflected. The values of the maximum lift coefficients (fig. 5) for both airfoils were substantially equivalent at corresponding flap deflections, but the angles of attack for maximum lift decreased as the flaps were deflected.

Deflecting the 0.15c drooped-nose flaps (fig. 6) increased the maximum section lift coefficients and increased the angles of attack for maximum lift primarily by alleviating the negative pressure peaks that cause leading-edge separation near maximum lift. These pressure peaks are alleviated because the flow approaching the leading edge is more nearly alined at high angles of attack when the drooped-nose flap is deflected. The maximum section lift coefficients for the 6- and 10-percent-thick airfoils at the optimum drooped-nose flap deflection of 30° are 1.17 and 1.15, respectively. At corresponding deflections of the 0.15c drooped-nose flap the maximum section lift coefficients of both airfoils are essentially the same. At angles of attack well below those for maximum lift the drooped-nose flaps act as spoilers on the lower surface of the airfoils and cause some reduction in lift. These losses in lift increase as the flap deflection is increased.

Extending the 0.10c leading-edge flaps (fig. 7) increased the maximum section lift coefficients and lift-curve slopes of both airfoils from the basic configurations. The higher slopes of the lift curves for the two airfoils with the 0.10c leading-edge flaps extended are primarily due to the fact that the section lift coefficients are based on the chord of the plain airfoil.

The variation of the increment in maximum section lift coefficient $\Delta c_{l_{max}}$ and increment in angle of attack at maximum lift $\Delta\alpha_{c_{l_{max}}}$ for both models with deflection of the drooped-nose flap and plain flap is summarized in figure 8. This figure clearly shows that the optimum drooped-nose flap deflection for maximum lift occurs at approximately 30° for both the 6- and the 10-percent-thick airfoils. No optimum deflection was obtained for the plain flap inasmuch as the highest test deflection was still the most effective. The maximum section lift coefficients of both airfoils are substantially equivalent at corresponding flap deflections, but the increments in maximum section lift coefficient with flap deflection

differ because of the lower maximum section lift coefficient of the 10-percent-thick airfoil with the flaps neutral. (See fig. 4.) As shown in figure 8, positive increments in the angle of attack at maximum lift resulted when the drooped-nose flap was deflected while negative increments were produced with the plain flap deflected.

The pitching-moment characteristics of the two models with any of the various types of flaps deflected (figs. 5 to 7) show that the aerodynamic center continues to move toward the leading edge as the high-lift device is put into operation. The area added to the leading edge of the basic model by extending the 0.10-chord leading-edge flap accounts for the usually large change in slope of the pitching-moment-coefficient curve inasmuch as the moments were measured about the quarter-chord point of the basic model.

Combined deflections of high-lift devices.- The results of tests of the two airfoils with various combinations of the high-lift devices are presented in figures 9 and 10. As shown in figure 9, the optimum flap deflections corresponding to the highest maximum section lift coefficient were $\delta_n = 30^\circ$, $\delta_f = 60^\circ$, and $\delta_n = 36^\circ$, $\delta_f = 60^\circ$ for the 6- and 10-percent-thick airfoils, respectively. The data for the 10-percent-thick airfoil with the plain flap deflected 60° indicate no important changes in the maximum section lift coefficient with small departures from the optimum drooped-nose-flap deflection.

A comparison between the lift characteristics of the two airfoils with the 0.15-chord drooped-nose flap deflected 30° and the 0.20-chord plain flap deflected 60° (fig. 9) with those for the airfoil with the plain flap deflected 60° (fig. 5) shows that the maximum section lift coefficients were increased 0.32 and 0.30 and the angles of attack for maximum lift were increased 6.5° and 6°, respectively, for the 6- and 10-percent-thick airfoils. A similar comparison between the lift characteristics of the two airfoils with the 0.10-chord leading-edge flap extended and the plain flap deflected 60° (fig. 10) with those for the two airfoils with the plain flap deflected 60° (fig. 5) shows that the maximum section lift coefficients were increased about 0.19 and 0.24 and the angles of attack for maximum lift were increased 1° and 2°, respectively, for the 6- and 10-percent-thick airfoils. A large percentage of these increases in maximum section lift coefficients is due to the increase in the model chords that occurs with the 0.10-chord leading-edge flaps extended since the coefficients are based on the chords of the basic models.

The section lift characteristics of the two airfoils with the drooped-nose and plain flaps deflected 30° and 60°, respectively, obtained at Reynolds numbers of 3×10^6, 6×10^6, and 9×10^6 are presented in figure 11. At Reynolds numbers between 3×10^6 and 9×10^6 the data (fig. 11(a)) show no appreciable scale effect on the maximum lift coefficient of the 6-percent-thick airfoil. In the case of the 10-percent thick airfoil (fig. 11(b)), however, some adverse scale effect is indicated in the maximum lift coefficient at Reynolds numbers between 3×10^6 and 6×10^6. Similarly, some adverse scale effect (fig. 9(c)) is indicated in the maximum lift coefficient at Reynolds numbers between 3×10^6 and 9×10^6 with the drooped-nose and plain flaps deflected 36° and 60°, respectively. At Reynolds numbers above 9×10^6, however, the maximum section lift coefficient of this combination remained approximately constant.

The section pitching-moment characteristics of the two airfoils at combined flap deflections of $\delta_n = 30^\circ$, $\delta_f = 60^\circ$ (fig. 11) show that the aerodynamic center remains ahead of the quarter-chord point. In addition, the combined action of the drooped-nose flap and plain flap caused the moment coefficients to increase negatively with increasing lift coefficient until the angle of attack was high enough that the spoiler action of the drooped-nose flap was alleviated. As the lift coefficient was increased beyond this point, the moment decreased negatively to approximately 2.5° beyond the angle of attack for maximum lift whereupon the moment curve breaks.

Low-drag-control flaps.- The lift and drag characteristics of the NACA 2S-(50)(03)-(50)(03) airfoil with the drooped-nose and plain flaps deflected are presented in figure 12. Deflecting the drooped-nose flap to 10° decreased the section drag coefficient of the 6-percent-thick circular-arc airfoil at a lift coefficient of 0.3 about 40 percent by delaying the formation of a negative pressure peak at the leading edge which causes separation. In general, deflecting the drooped-nose flap was more effective in extending the low-drag range to higher section lift coefficients than was deflecting the plain flap.

CONCLUSIONS

A two-dimensional wind-tunnel investigation was made of symmetrical circular-arc airfoils, 6 and 10 percent thick, with

leading-edge and trailing-edge high-lift devices at Reynolds numbers from 2.1×10^6 to 18×10^6. The results obtained indicated the following conclusions:

1. Maximum lift coefficients of 1.95 and 2.03 were obtained for the optimum combination of drooped-nose and plain flaps for the 6- and 10-percent-thick airfoils, respectively. The corresponding maximum lift coefficients for the plain airfoils were 0.73 and 0.67, respectively.

2. The optimum combination of flap deflections for the 6- and 10-percent-thick airfoils were found to be $\delta_n = 30^\circ$, $\delta_f = 60^\circ$, and $\delta_n = 36^\circ$, $\delta_f = 60^\circ$, respectively, where δ_n represents the drooped-nose and δ_f the plain-flap deflections. The results for the 10-percent-thick airfoil with the plain flap deflected 60° indicate no important changes in the maximum section lift coefficient with small departures from the optimum drooped-nose-flap deflection.

3. The scale effects on the maximum lift coefficient were, in general, negligible.

4. The section pitching-moment characteristics indicated that the aerodynamic center was ahead of the quarter-chord point and moved toward the leading edge when any of the high-lift devices was deflected or extended.

5. Deflecting the drooped-nose flap was more effective in extending the low-drag range to higher section lift coefficients than deflecting the plain flap.

Langley Memorial Aeronautical Laboratory
National Advisory Committee for Aeronautics
Langley Field, Va.

REFERENCES

1. Abbott, Ira H., von Doenhoff, Albert E., and Stivers, Louis S., Jr.: Summary of Airfoil Data. NACA ACR No. L5C05, 1945.

2. Purser, Paul E., and Johnson, Harold S.: Effects of Trailing-Edge Modifications on Pitching-Moment Characteristics of Airfoils. NACA CB No. L4130, 1944.

TABLE I
ORDINATES FOR THE NACA 2S-(50)(03)-(50)(03)
AIRFOIL

Stations and ordinates given in percent of airfoil chord

Upper surface		Lower surface	
Station	Ordinate	Station	Ordinate
0	0	0	0
5	.572	5	-.572
10	1.082	10	-1.082
15	1.533	15	-1.533
20	1.922	20	-1.922
25	2.252	25	-2.252
30	2.521	20	-2.521
35	2.731	35	-2.731
40	2.880	40	-2.880
45	2.970	45	-2.970
50	3.000	50	-3.000
55	2.970	55	-2.970
60	2.880	60	-2.880
65	2.731	65	-2.731
70	2.521	70	-2.521
75	2.252	75	-2.252
80	1.922	80	-1.922
85	1.533	85	-1.533
90	1.082	90	-1.082
95	.572	95	-.572
100	0	100	0
Radius of circular arc: 4.182 c			

NATIONAL ADVISORY
COMMITTEE FOR AERONAUTICS

TABLE II
ORDINATES FOR THE NACA 2S-(50)(05)-(50)(05)
AIRFOIL

Stations and ordinates given in percent of airfoil chord

Upper surface		Lower surface	
Station	Ordinate	Station	Ordinate
0	0	0	0
5	.958	5	-.958
10	1.812	10	-1.812
15	2.562	15	-2.562
20	3.211	20	-3.211
25	3.759	25	-3.759
30	4.207	30	-4.207
35	4.554	35	-4.554
40	4.802	40	-4.802
45	4.951	45	-4.951
50	5.000	50	-5.000
55	4.951	55	-4.951
60	4.802	60	-4.802
65	4.554	65	-4.554
70	4.207	70	-4.207
75	3.759	75	-3.759
80	3.211	80	-3.211
85	2.562	85	-2.562
90	1.812	90	-1.812
95	.958	95	-.958
100	0	100	0
Radius of circular arc: 2.525 c			

NATIONAL ADVISORY
COMMITTEE FOR AERONAUTICS

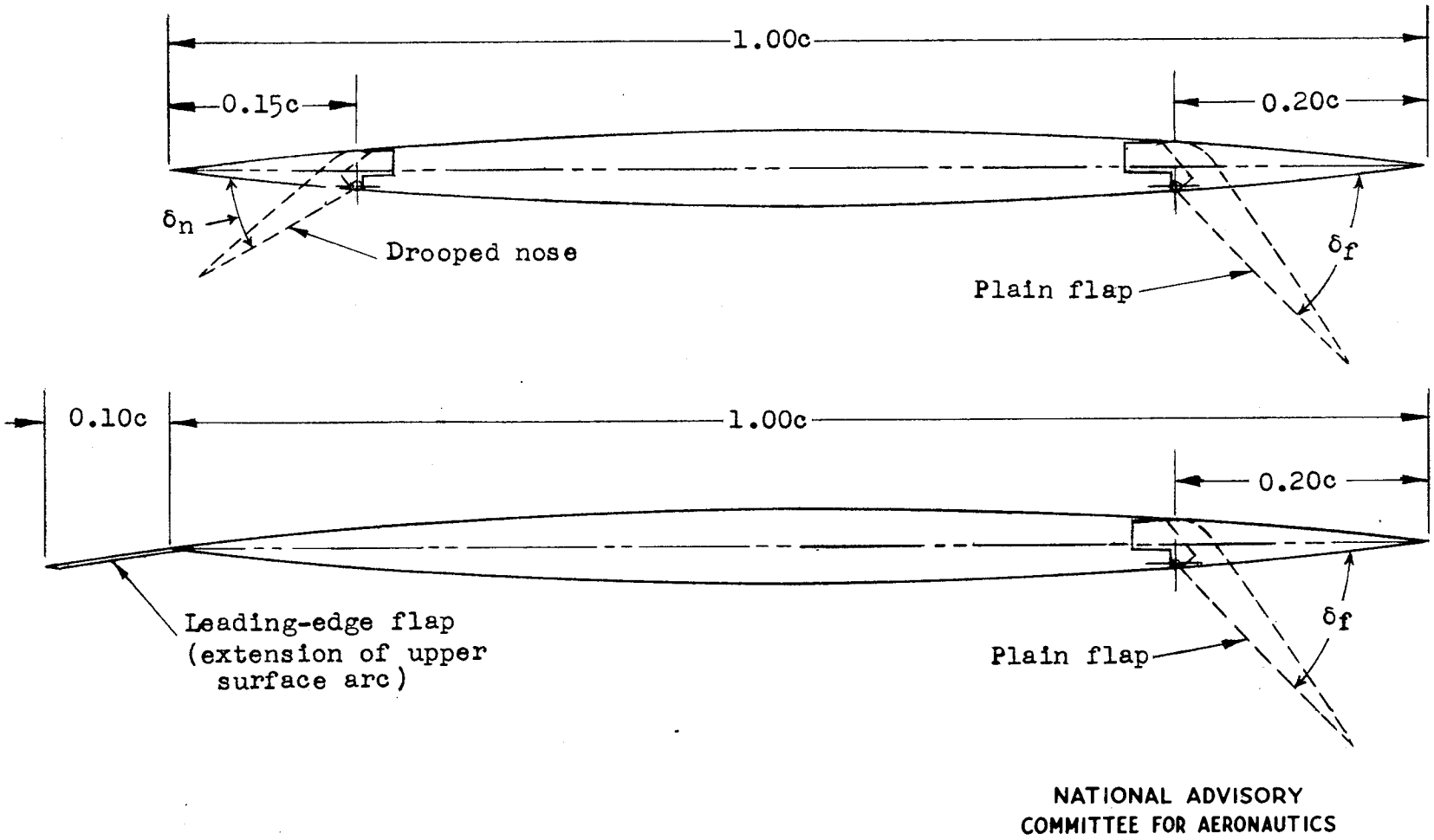

(a) NACA 2S-(50)(03)-(50)(03).

Figure 1.- Symmetrical circular-arc airfoils with leading-edge and trailing-edge high-lift devices.

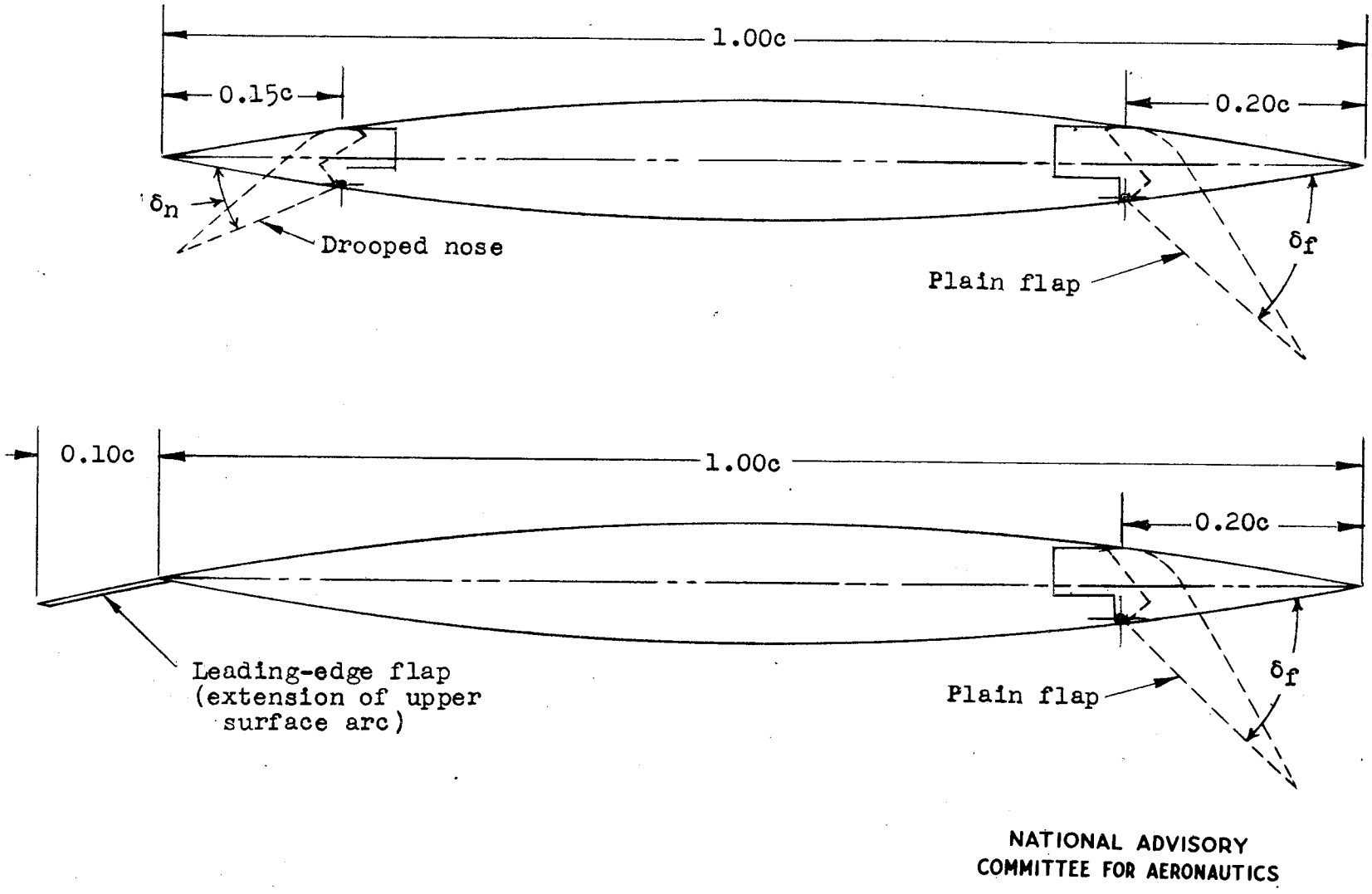

(b) NACA 2S-(50)(05)-(50)(05).

Figure 1.- Concluded.

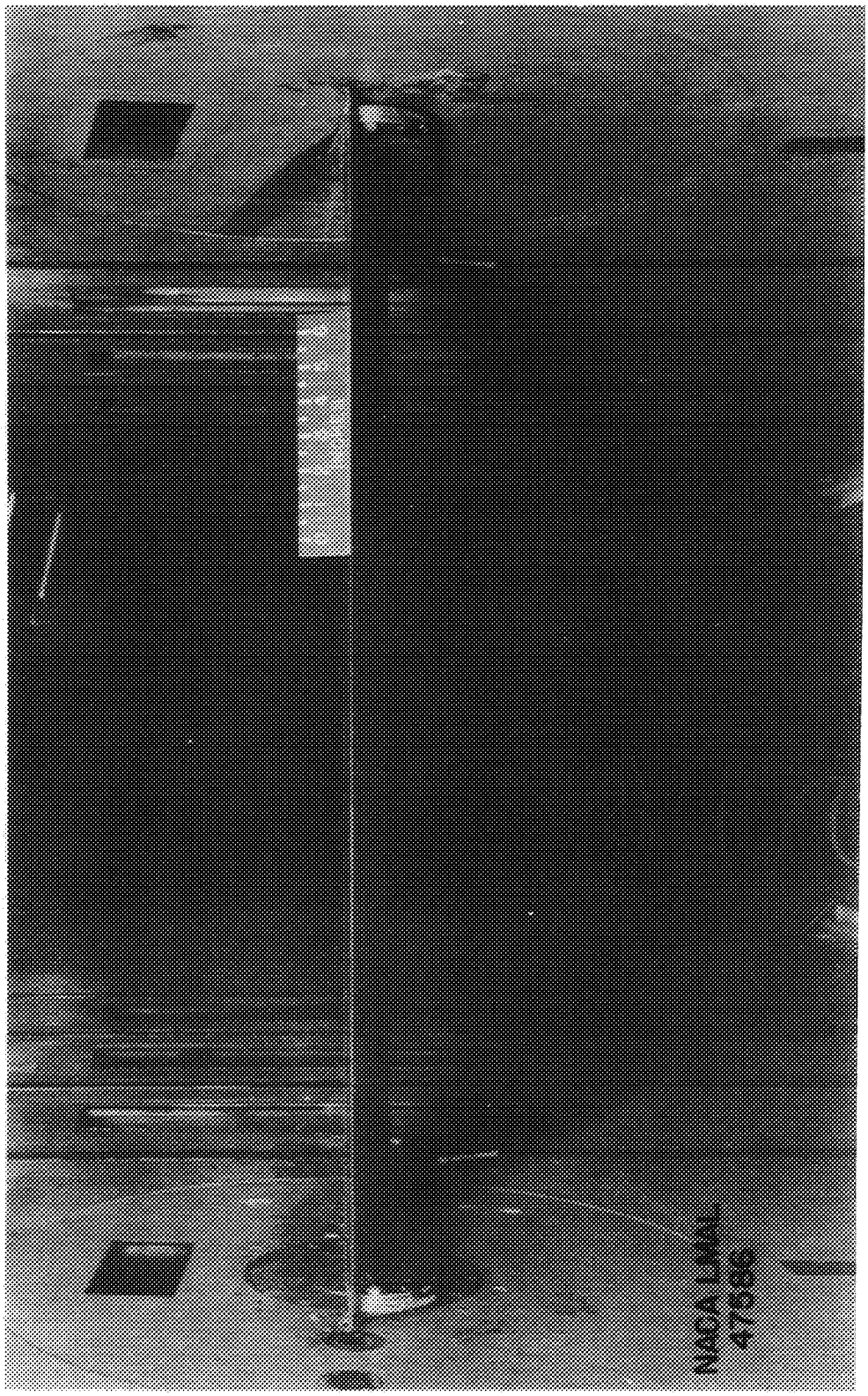

Figure 2.- Front view of a symmetrical circular-arc airfoil equipped with end plates.

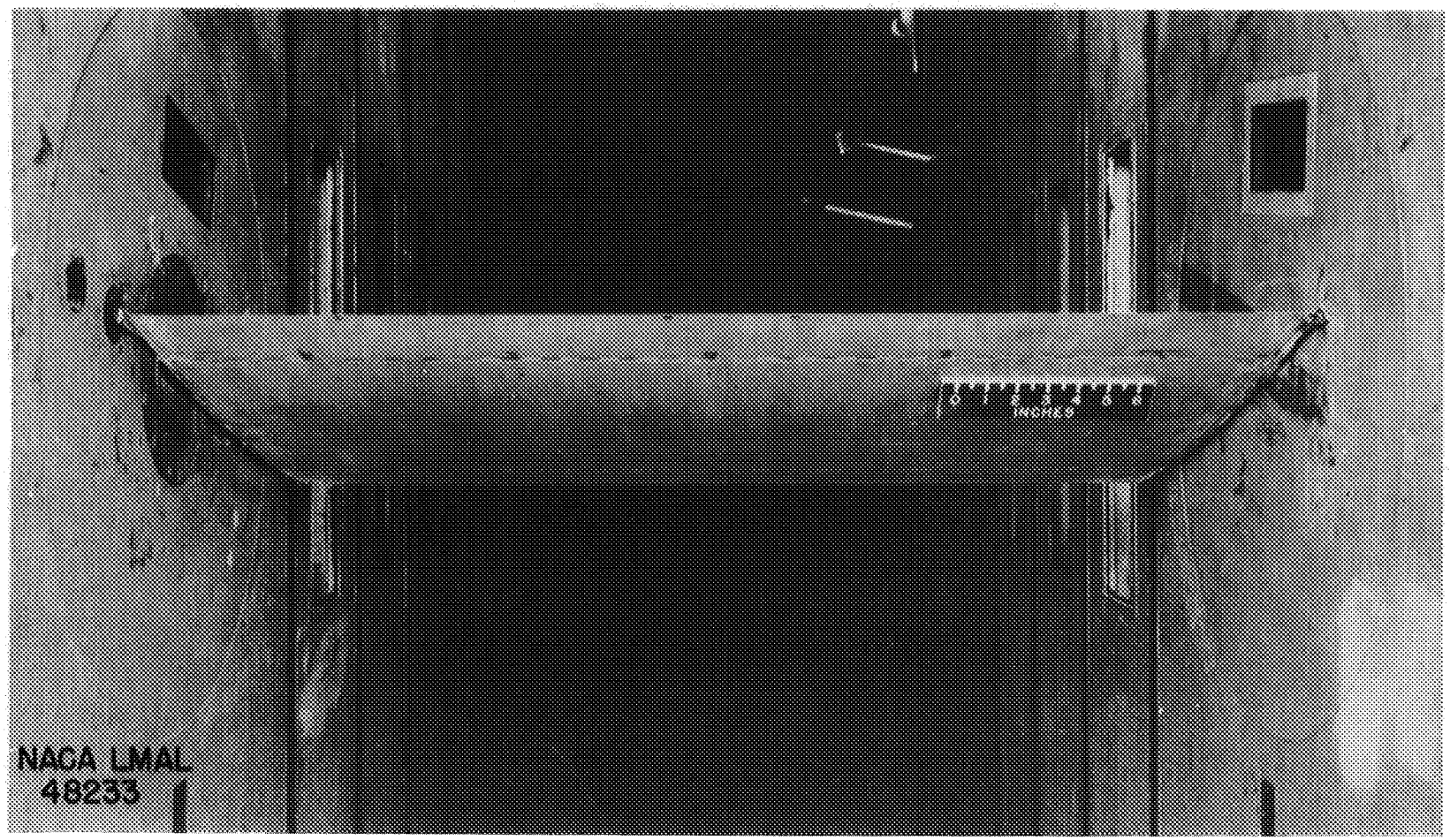

Figure 3.- Front view of a symmetrical circular-arc airfoil without end plates.

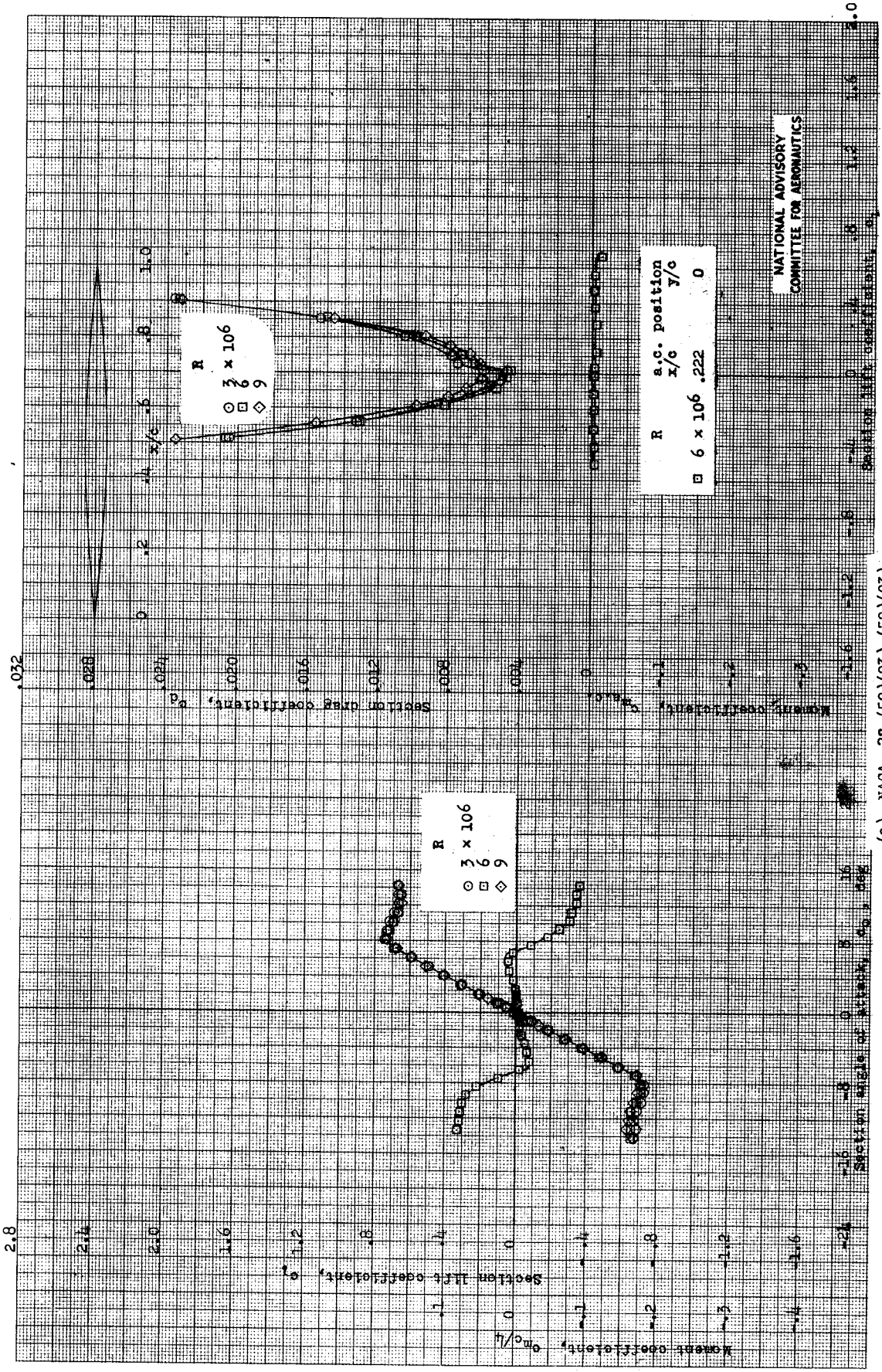

(a) NACA 2S-(50)(03)-(50)(03).

Figure 4.- Aerodynamic characteristics of two symmetrical circular-arc airfoils.

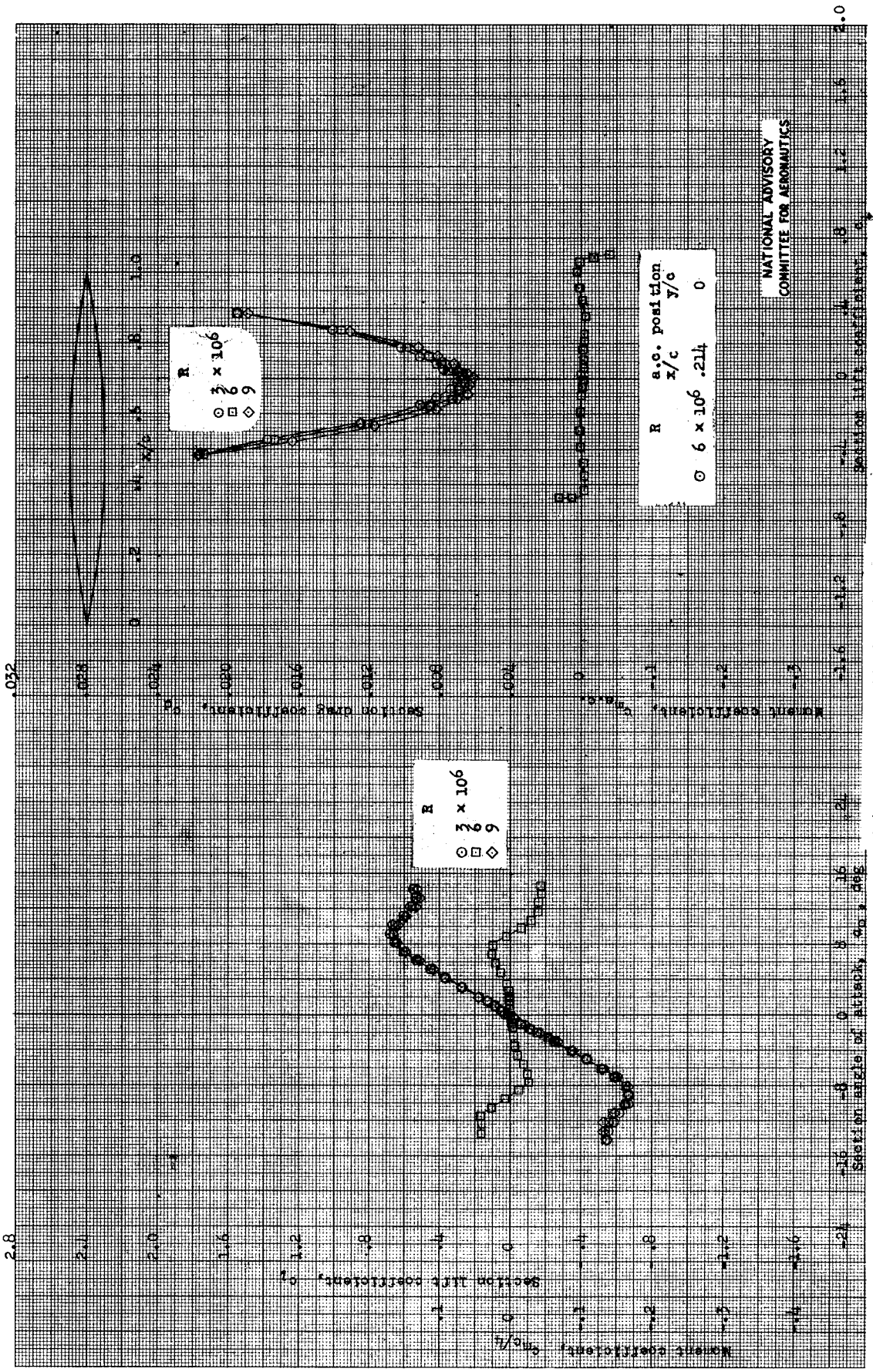

(b) NACA 2S-(50)(05)-(50)(05).

Figure 4.- Continued.

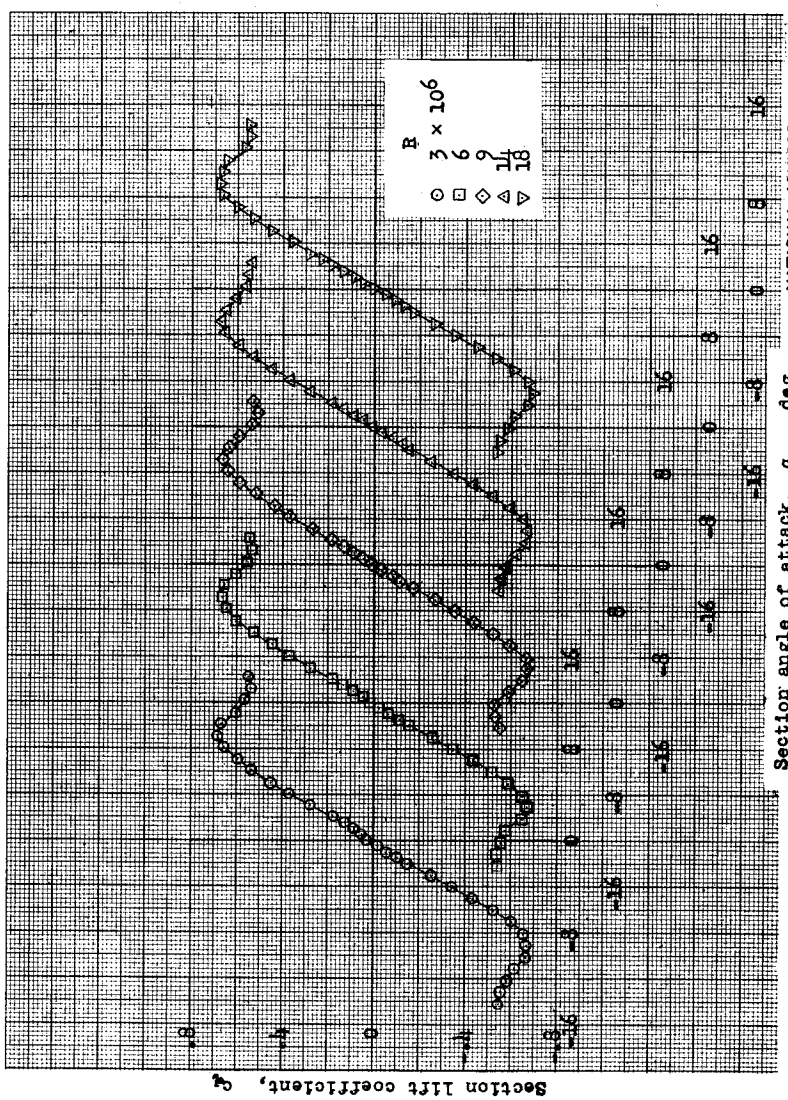

(c) NACA 28-(50)(05)-(50)(05)

Figure 4.- Concluded.

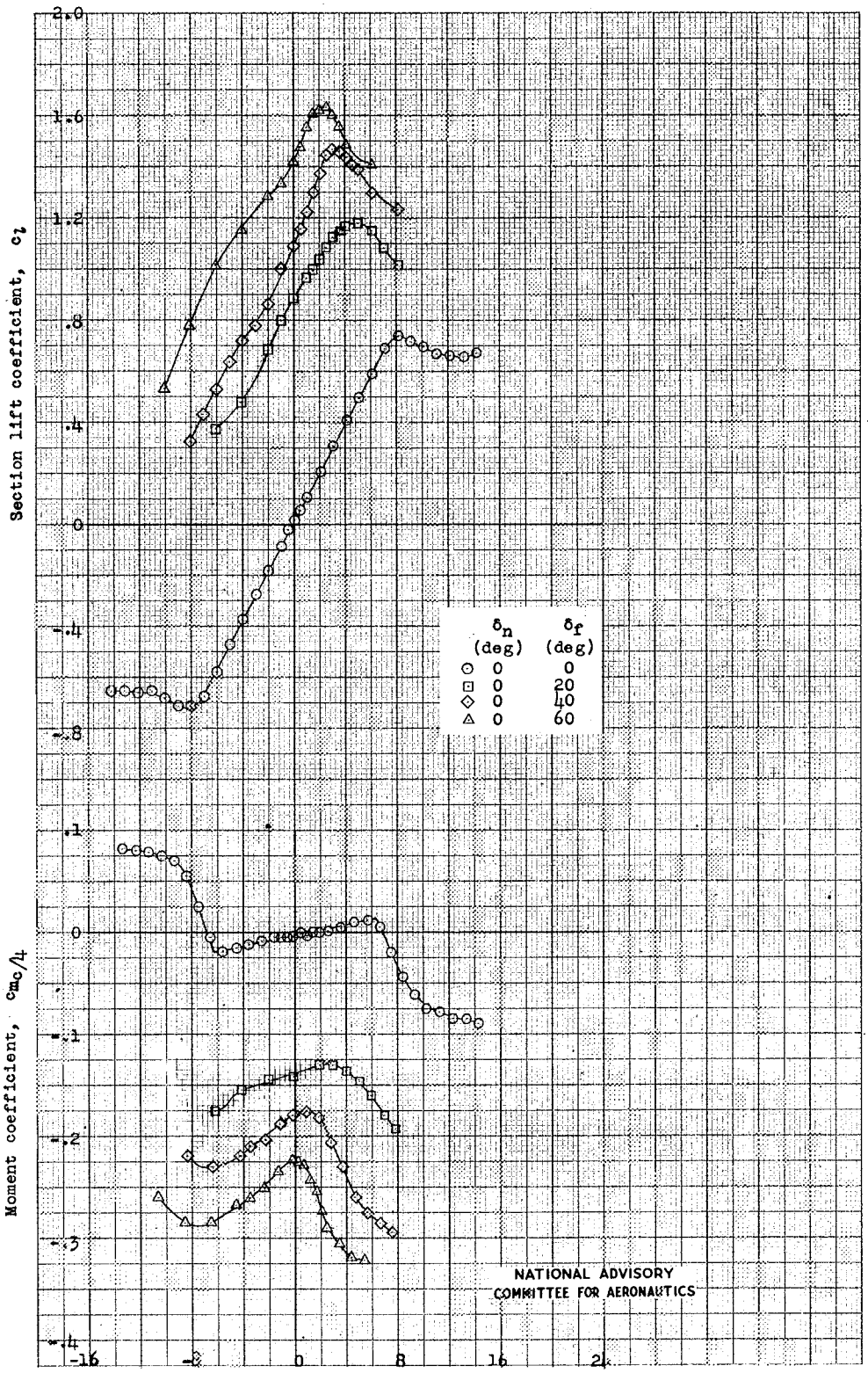

(a) NACA 2S-(50)(03)-(50)(03).

Figure 5.- Section lift and pitching-moment characteristics of two symmetrical circular-arc airfoils for various deflections of the 0.20-chord plain flap; R, 6×10^6.

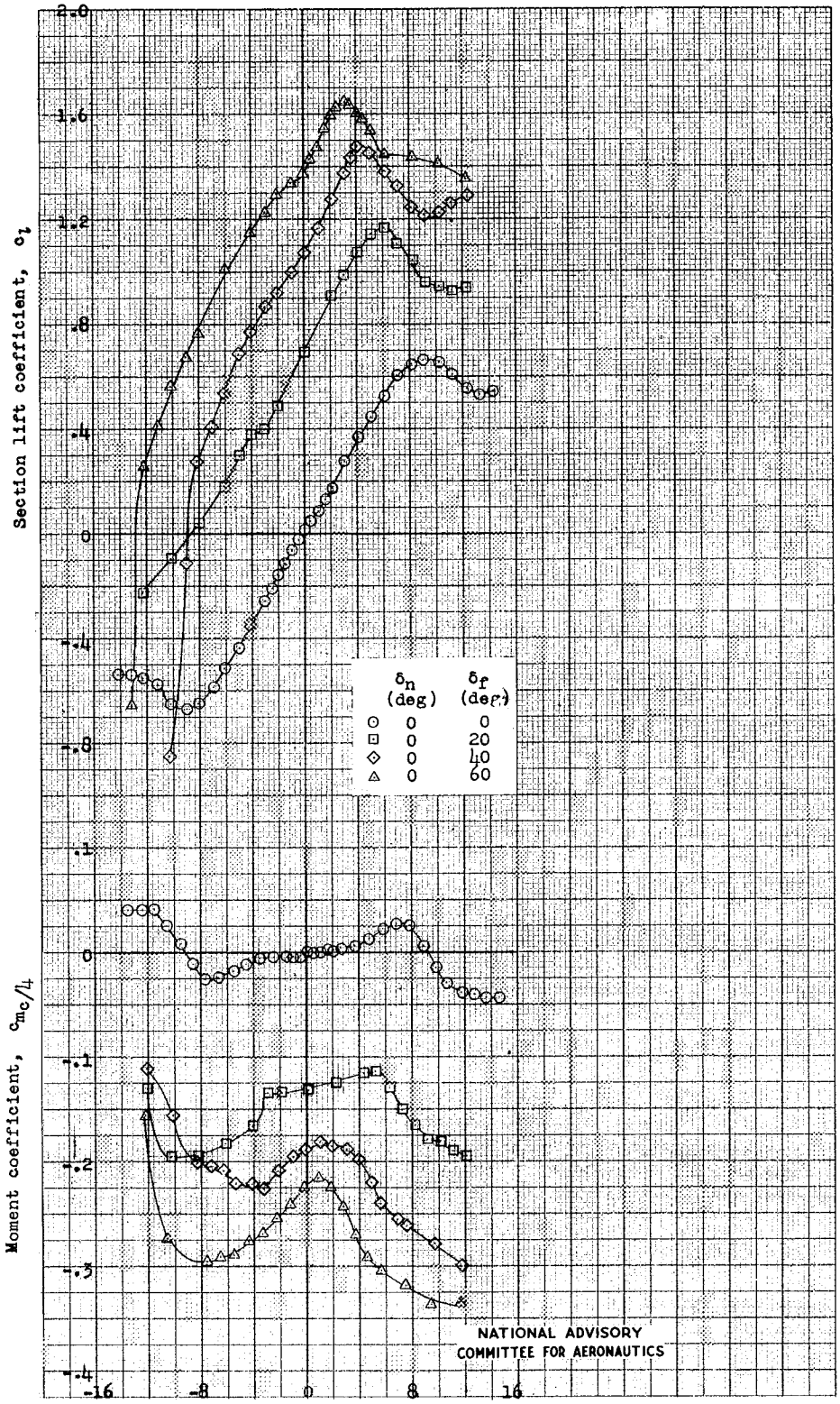

Section angle of attack, α_o, deg

(b) NACA 2S-(50)(05)-(50)(05).

Figure 5.- Concluded.

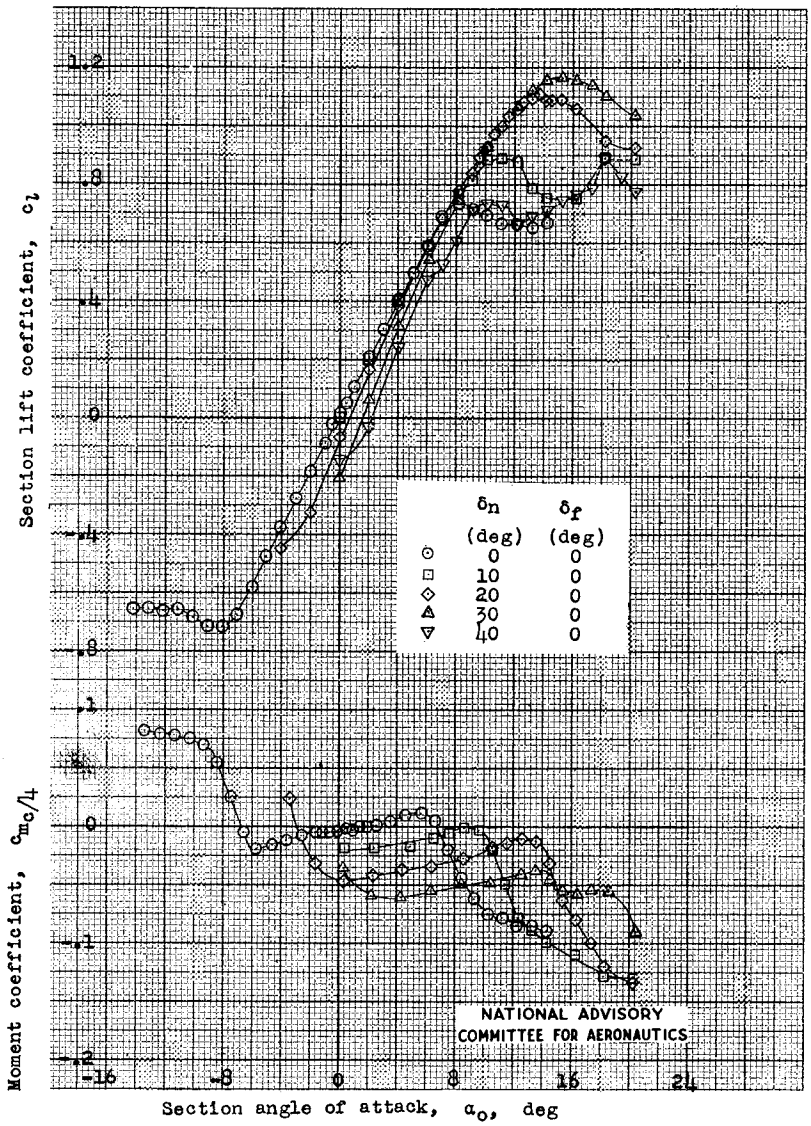

(a) NACA 2S-(50)(03)-(50)(03).

Figure 6.- Section lift and pitching-moment characteristics of two symmetrical circular-arc airfoils for various deflections of the 0.15-chord drooped-nose flap; R, 6×10^6.

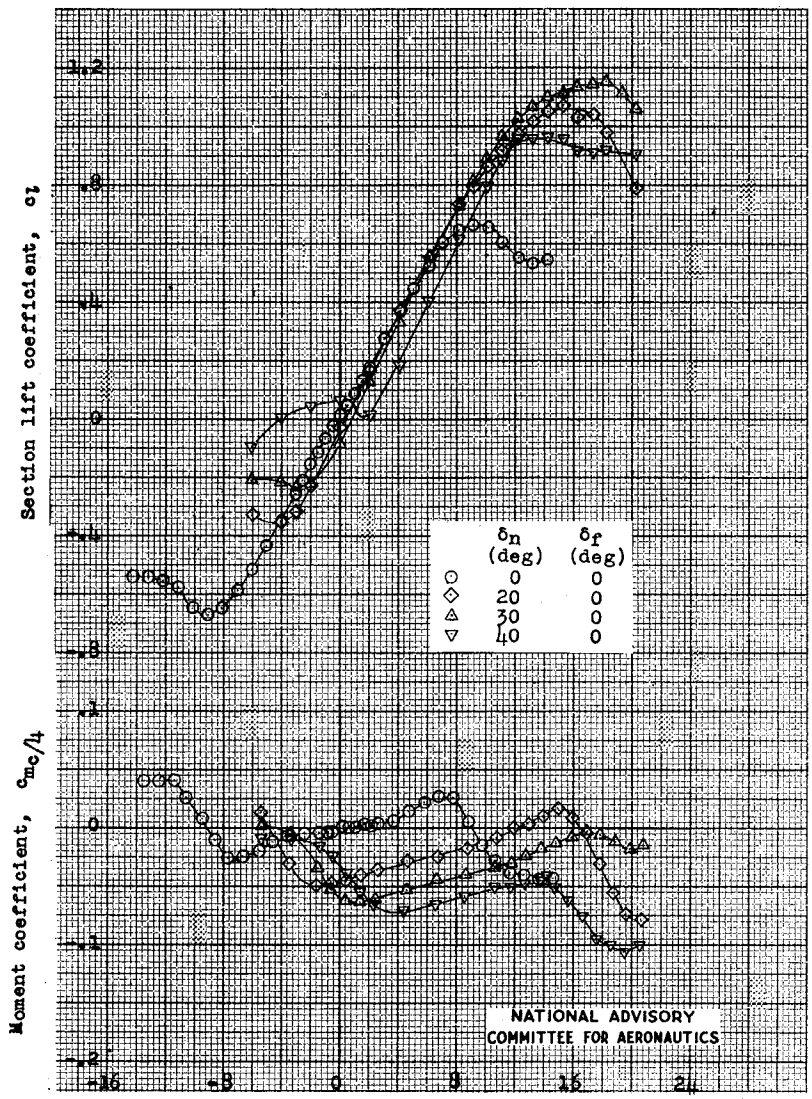

(b) NACA 2S-(50)(05)-(50)(05).

Figure 6.- Concluded.

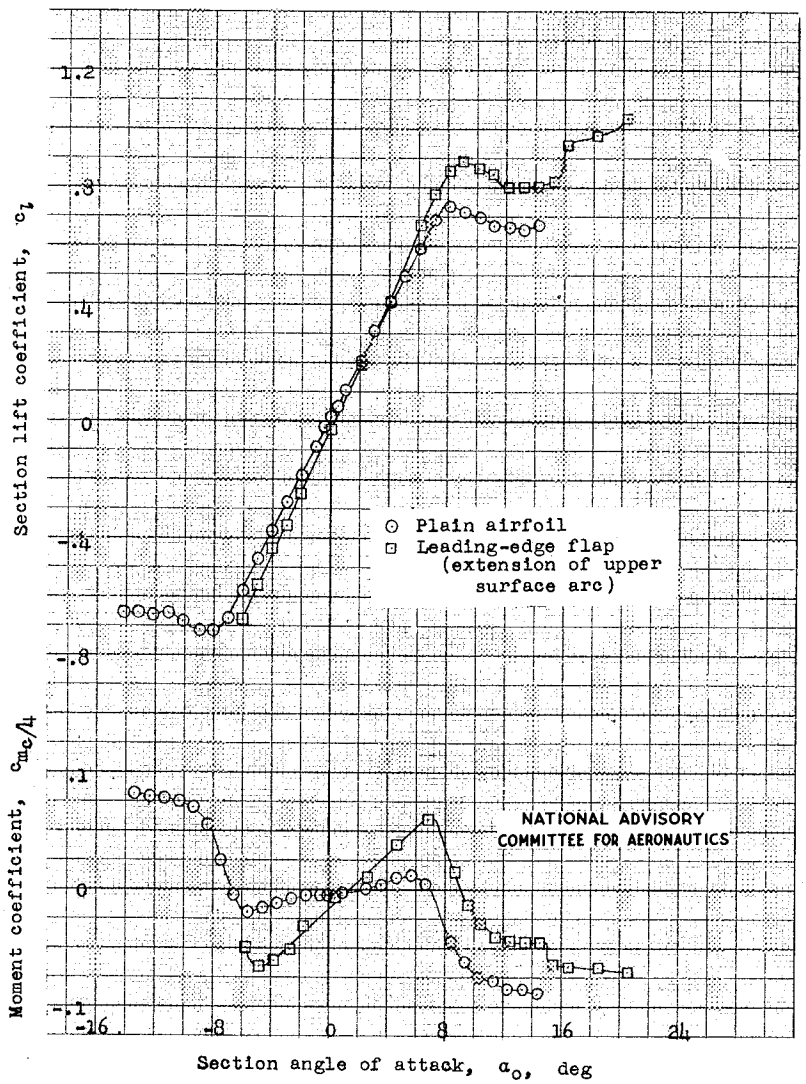

(a) NACA 2S-(50)(03)-(50)(03).

Figure 7.- Section lift and pitching-moment characteristics of two symmetrical circular-arc airfoils with and without the 0.10-chord extensible leading-edge flap; R, 6×10^6.

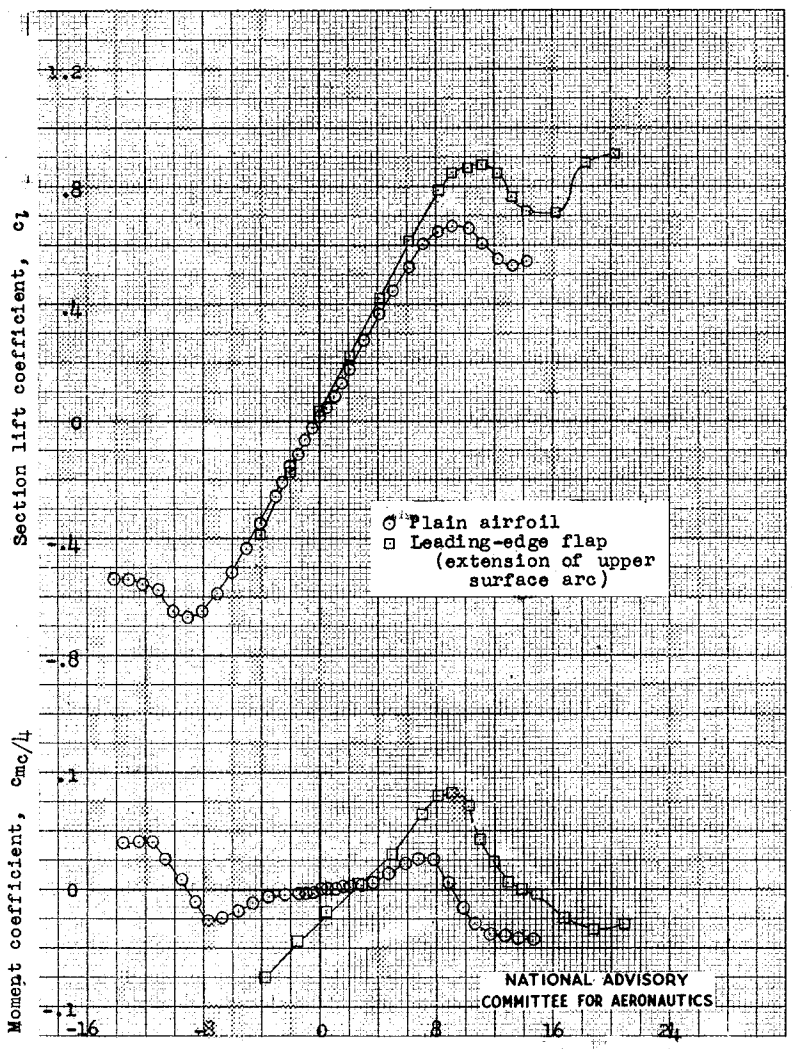

(b) NACA 2S-(50)(05)-(50)(05).

Figure 7.- Concluded.

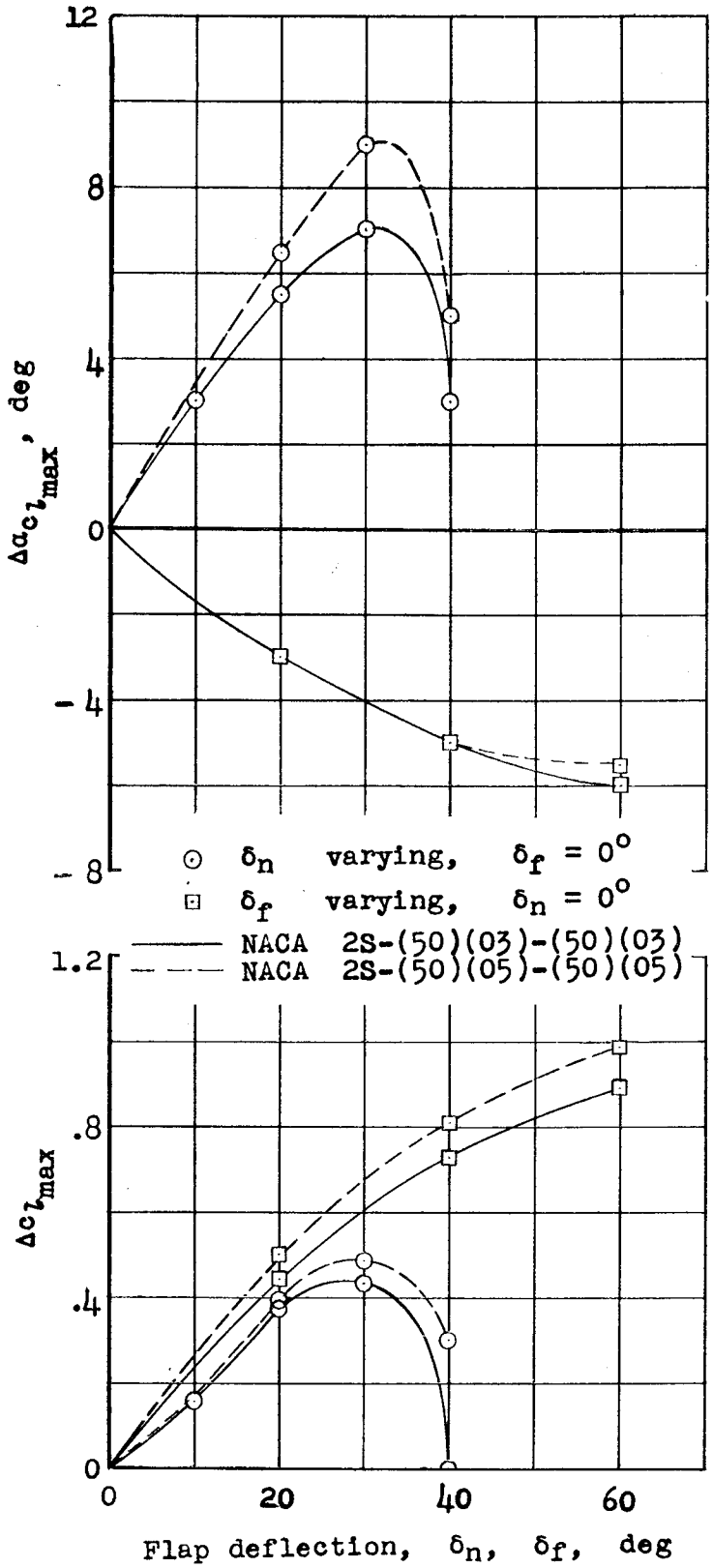

Figure 8.- Variation of the increment in maximum section lift coefficient and angle of stall with deflection of the drooped-nose and plain flaps; R, 6×10^6.

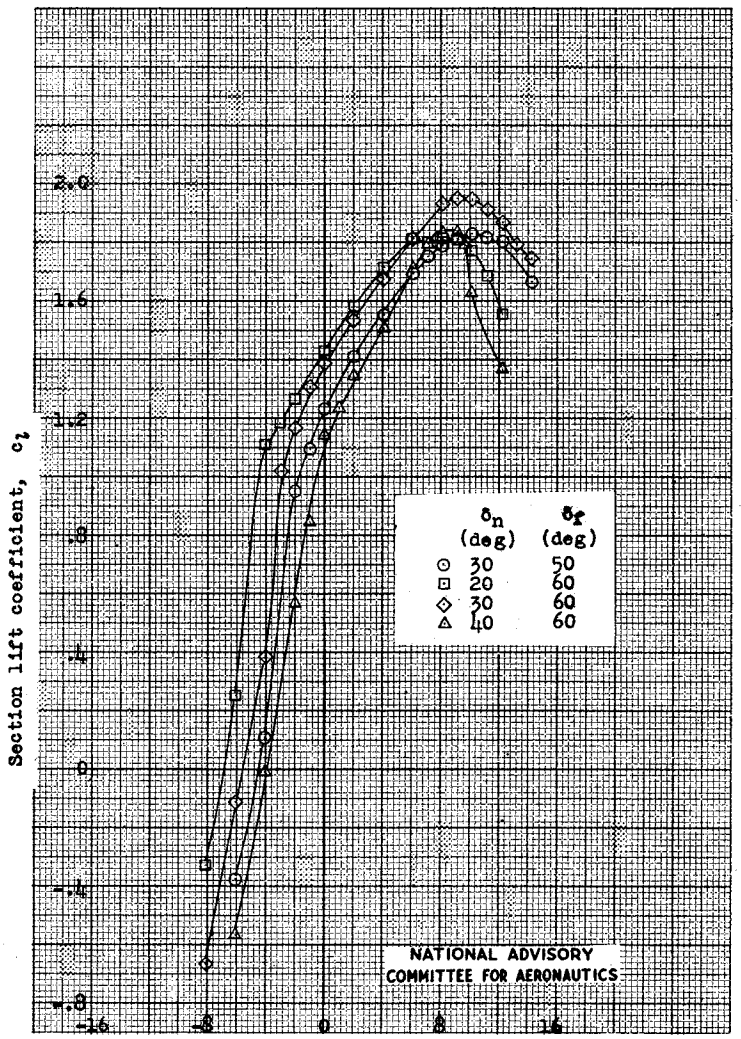

(a) NACA 2S-(50)(03)-(50)(03).

Figure 9.- Section lift characteristics of two symmetrical circular-arc airfoils for various deflections of the drooped-nose and plain flaps; R, 6×10^6.

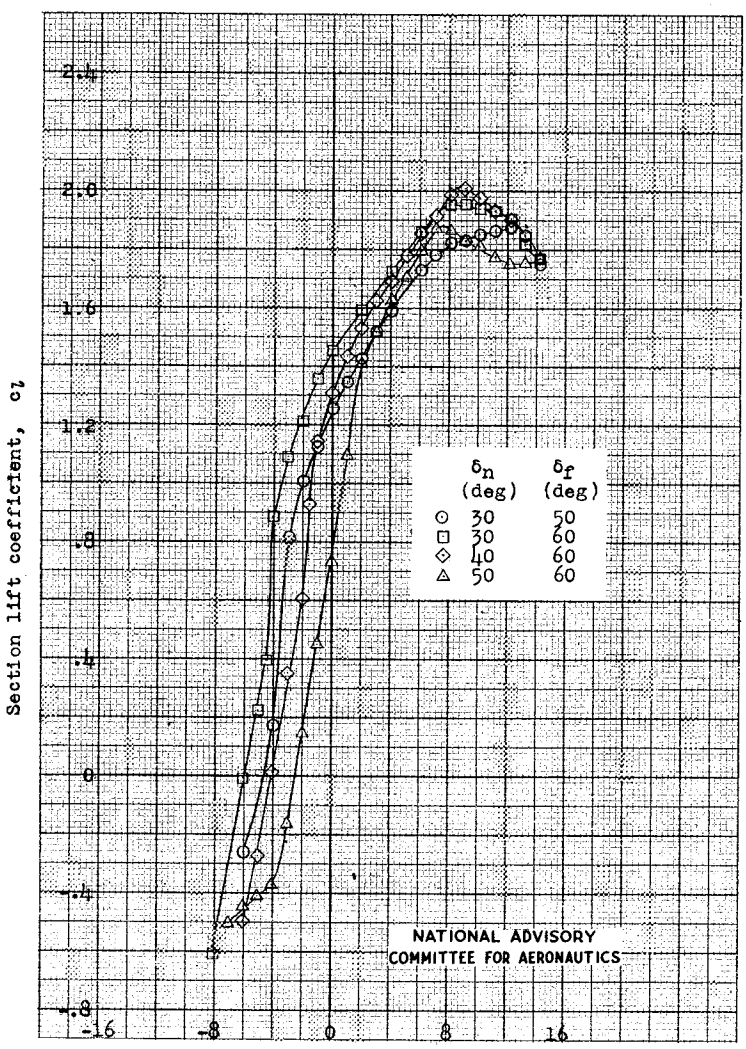

(b) NACA 2S-(50)(05)-(50)(05).

Figure 9.- Continued.

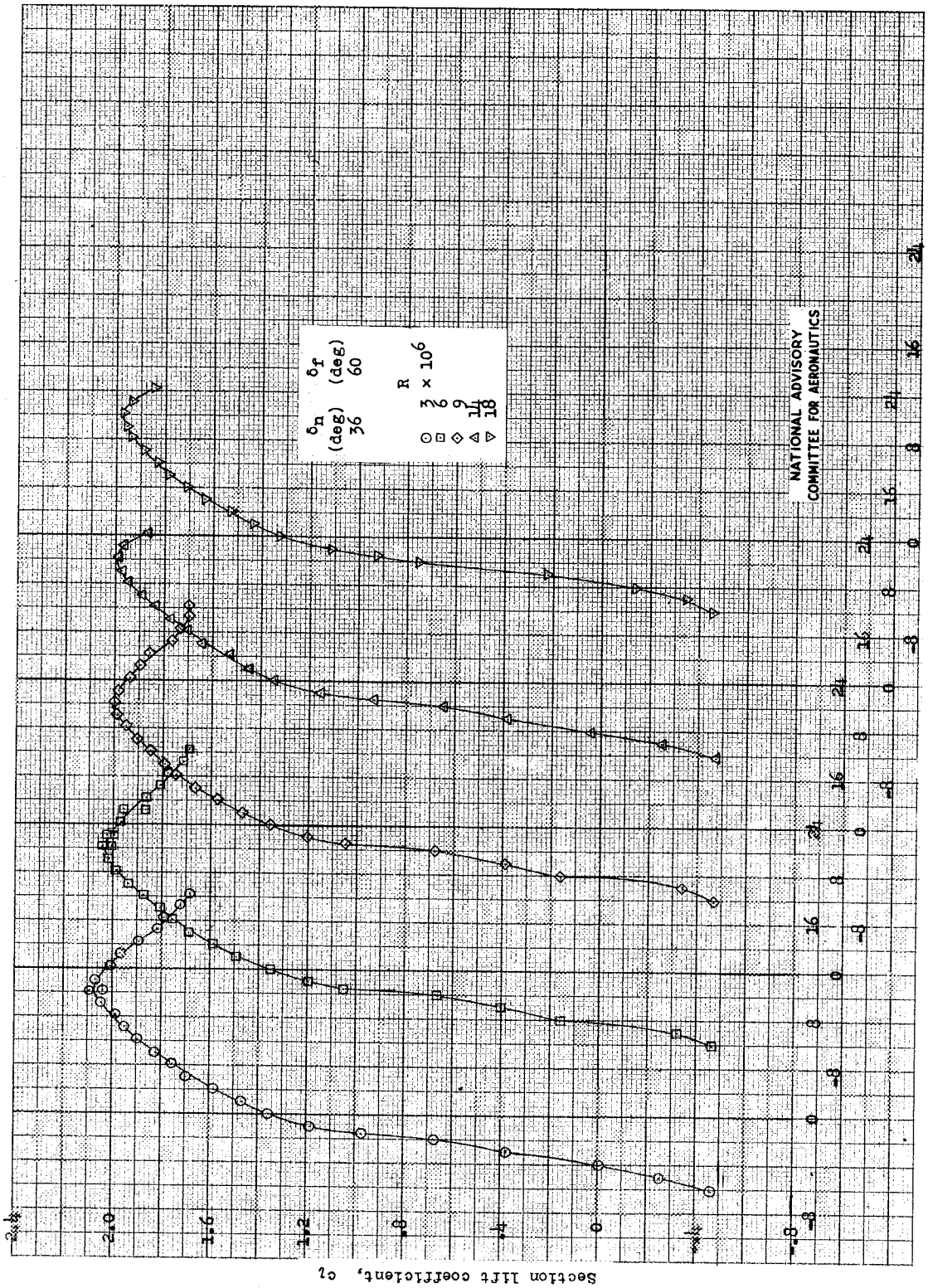

(c) NACA 2S-(50)(05)-(50)(05)

Figure 9.- Concluded.

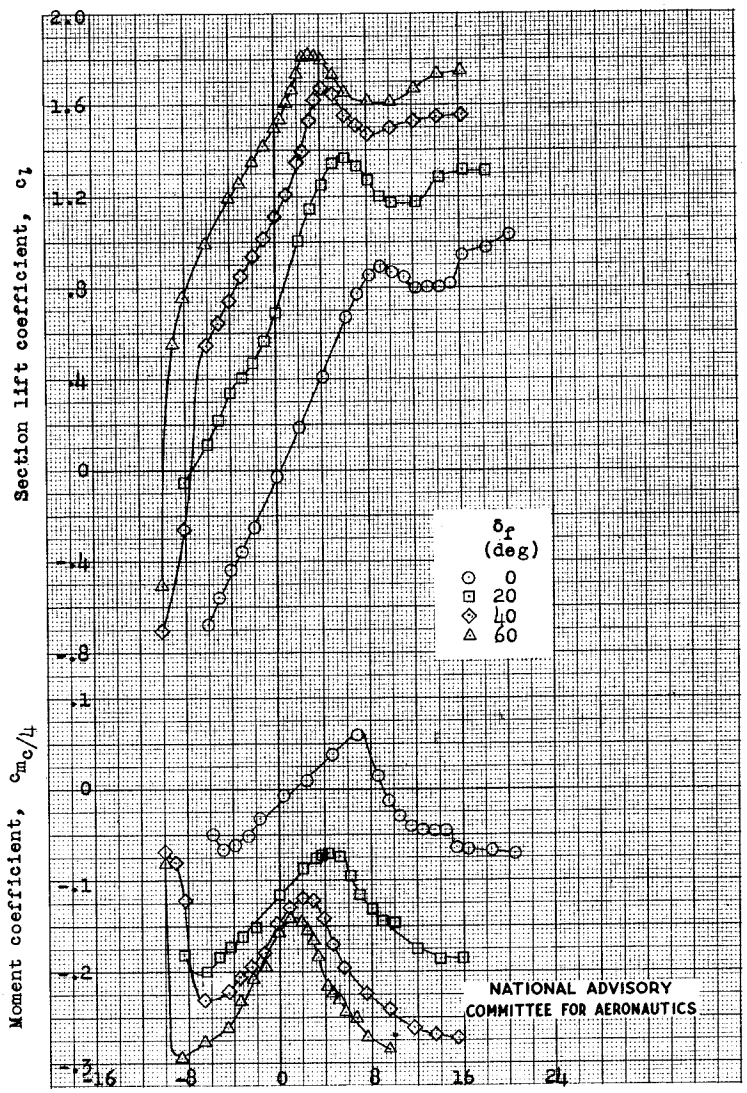

(a) NACA 2S-(50)(03)-(50)(03).

Figure 10.- Section lift and pitching-moment characteristics of two symmetrical circular-arc airfoils with the 0.10-chord extensible leading-edge flap and the 0.20-chord plain flap; R, 6×10^6.

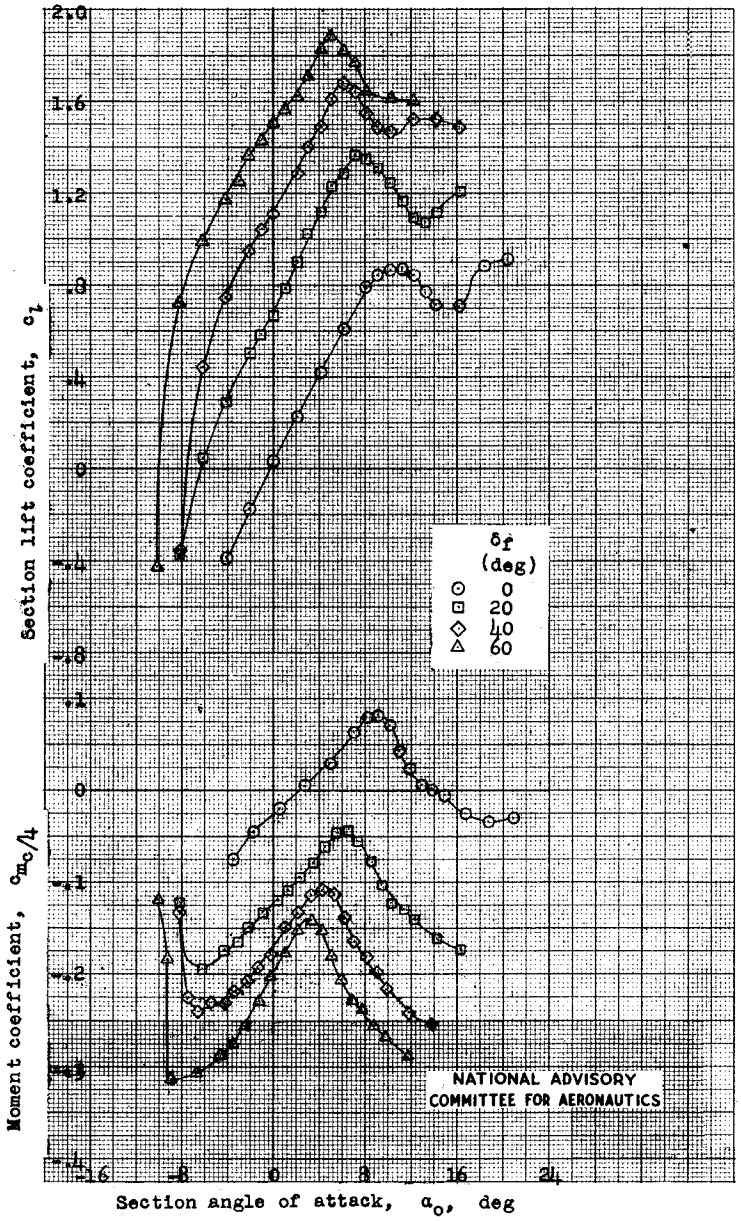

(b) NACA 2S-(50)(05)-(50)(05).

Figure 10.- Concluded.

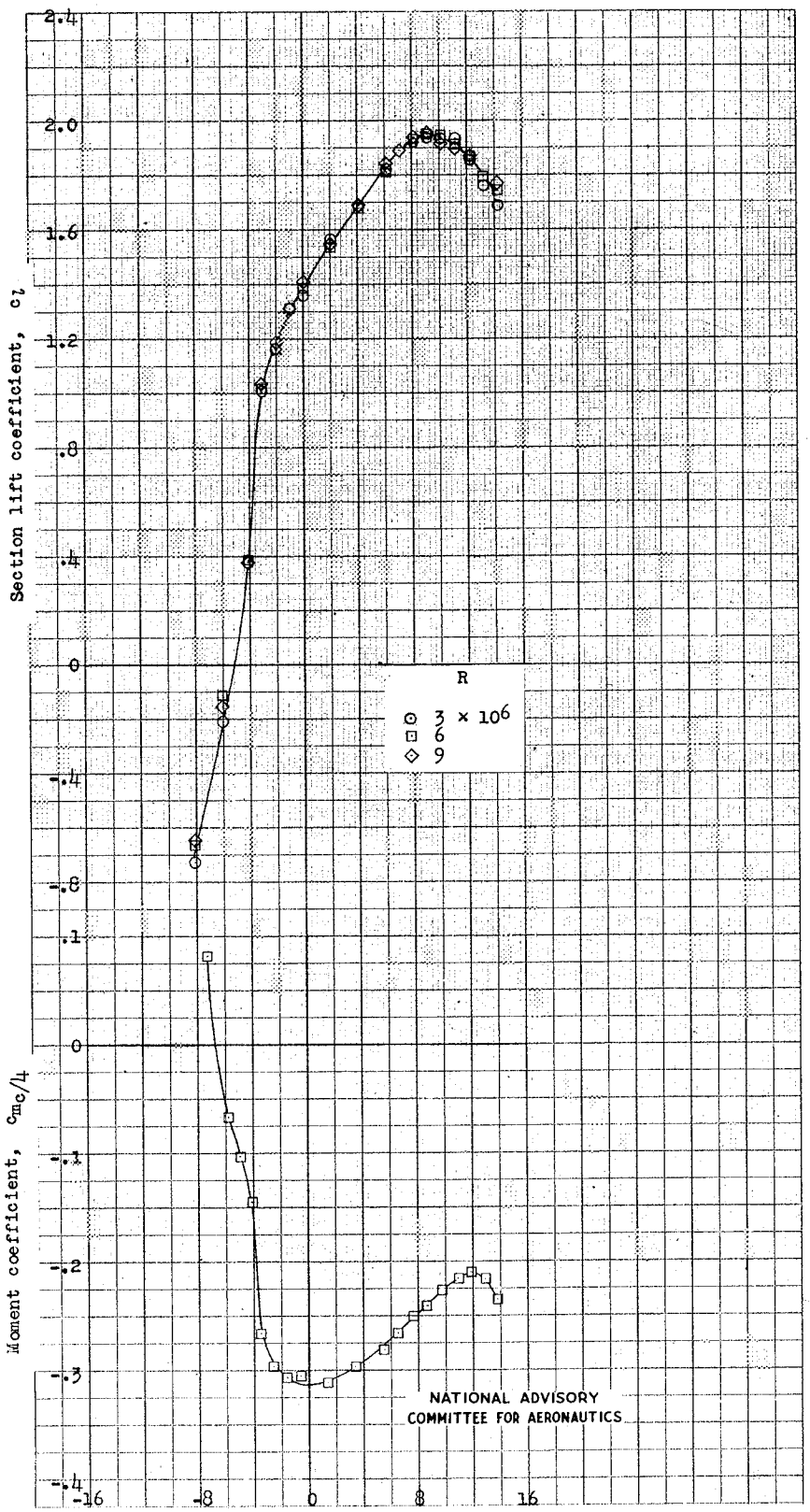

(a) NACA 2S-(50)(03)-(50)(03).

Figure 11.- Section lift and pitching-moment characteristics of two symmetrical circular-arc airfoils with the drooped-nose flap deflected 30° and the plain flap deflected 60°.

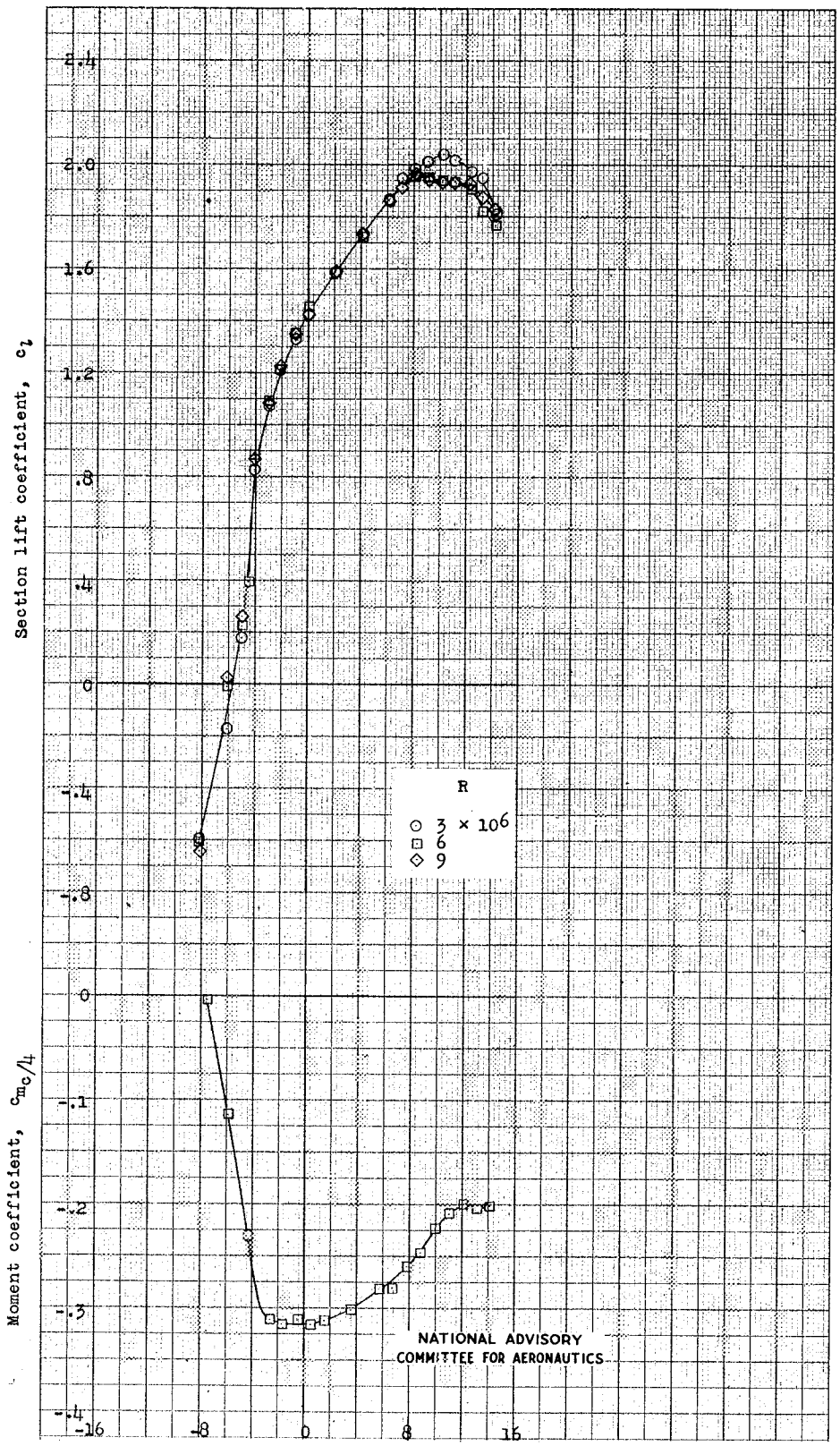

(b) NACA 2S-(50)(05)-(50)(05).

Figure 11.- Concluded.

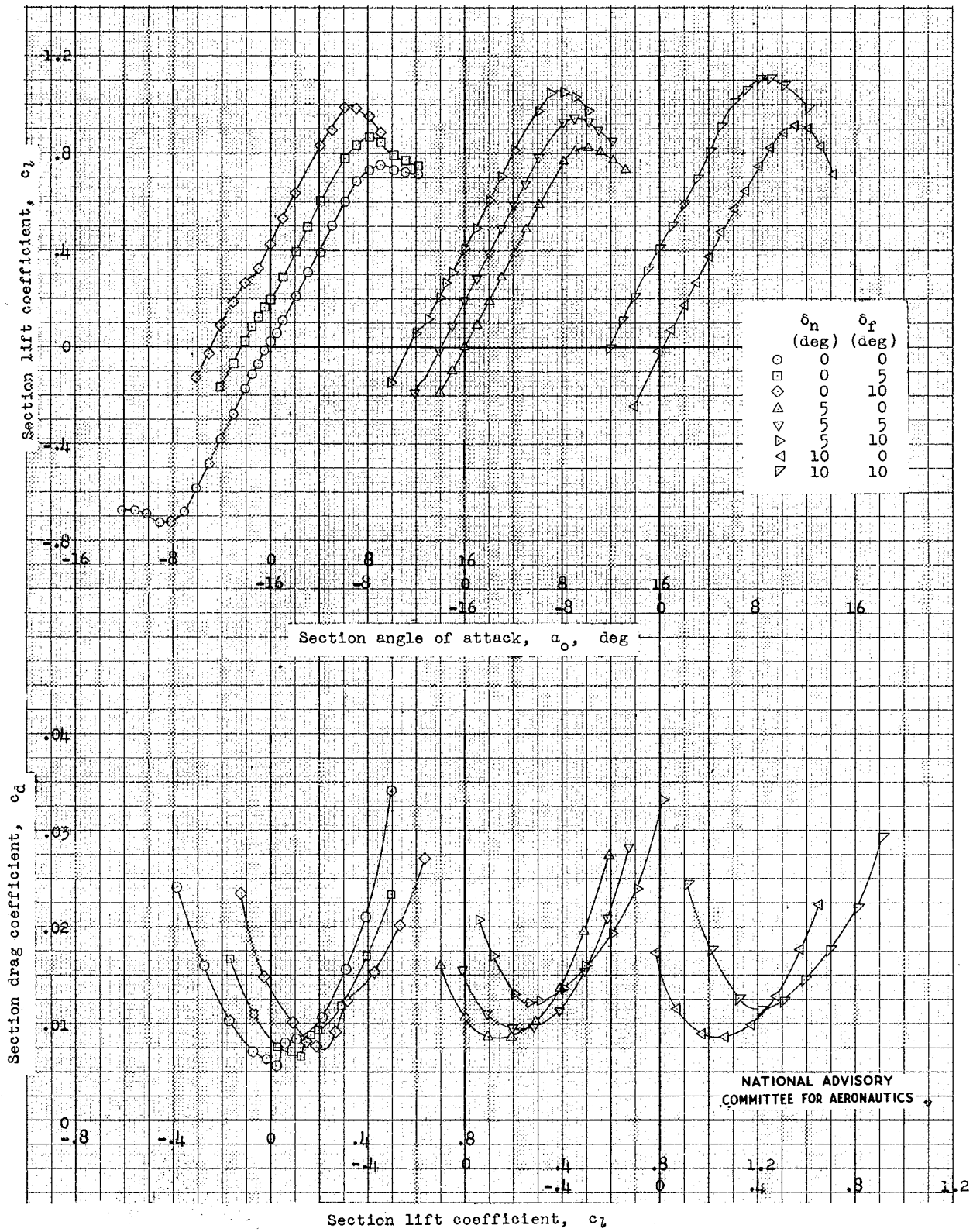

Figure 12.- Section lift and drag characteristics of an NACA 2S-(50)(03)-(50)(03) airfoil for various deflections of the drooped-nose and plain flaps; R, 2.1×10^6.